Porphyrin Sensitizers

DOI: 10.1002/anie.201309343

Molecular Engineering of Push–Pull Porphyrin Dyes for Highly Efficient Dye-Sensitized Solar Cells: The Role of Benzene Spacers**

Aswani Yella, Chi-Lun Mai, Shaik M. Zakeeruddin, Shu-Nung Chang, Chi-Hung Hsieh, Chen-Yu Yeh, and Michael Grätzel**

Abstract: *Porphyrins have drawn much attention as sensitizers owing to the large absorption coefficients of their Soret and Q bands in the visible region. In a donor and acceptor zinc porphyrin we applied a new strategy of introducing 2,1,3-benzothiadiazole (BTD) as a π-conjugated linker between the anchoring group and the porphyrin chromophore to broaden the absorption spectra to fill the valley between the Soret and Q bands. With this novel approach, we observed 12.75% power-conversion efficiency under simulated one-sun illumination (AM1.5G, 100 mW cm^{-2}). In this study, we showed the importance of introducing the phenyl group as a spacer between the BTD and the zinc porphyrin in achieving high power-conversion efficiencies. Time-resolved fluorescence, transient-photocurrent-decay, and transient-photovoltage-decay measurements were employed to determine the electron-injection dynamics and the lifetime of the photogenerated charge carriers.*

Because of the increasing demand for energy worldwide and global warming, the development of renewable energy sources is required to enable reduced consumption of fossil fuels. In the field of solar-energy conversion into electricity, dye-sensitized solar cells (DSCs) have attracted considerable attention owing to their low cost and high efficiency.[1] DSCs based on ruthenium sensitizers have reached overall solar-to-electric power-conversion efficiency (PCE) of 11.4% under standard air mass 1.5 G illumination.[2–6] For reasons of availability and cost, it is important to develop efficient noble-metal-free sensitizers. Much effort has been devoted to the development of donor–π-acceptor (D–π-A) organic sensitizers, which currently reach more than 10% PCE.[7–11] Porphyrins have drawn much attention as sensitizers as a result of the large absorption coefficients of their Soret and Q-bands in the visible region. It is possible to tune the spectral properties and energetics of porphyrins by functionalization at the *meso* and β positions of the chromophore.[12–19] The strategy of introducing donor and acceptor moieties at the periphery and using a zinc porphyrin chromophore as a π bridge has produced a whole new family of efficient sensitizers by creating judicious directional electron flow from the donor to the acceptor moiety, which anchors the dye to the surface of the oxide scaffold acting as the electron acceptor.[20–25] Recently, a PCE of 12.3% was reached by combining a donor–acceptor zinc porphyrin with an organic cosensitizer dye and using a cobalt complex as a redox shuttle in the electrolyte.[26] The cosensitization approach is effective in promoting a broad absorption spectral response; the device performance is enhanced through the application of two dyes containing complimentary absorption spectra. Previously, we successfully utilized 2,1,3-benzothiadiazole as an electron acceptor to develop highly efficient organic dyes.[27] Herein we report a novel molecular design of a donor–acceptor porphyrin dye. The introduction of an electron acceptor as a π-conjugated linker in between the anchoring group and the porphyrin chromophore led to a broadening of the absorption to partially fill the valley between the Soret and Q-bands. With this new strategy, we observed 12.75% efficiency with a single porphyrin dye containing 2,1,3-benzothiadiazole (BTD) as an electron acceptor π-conjugated with benzoic acid as an anchoring group. We also investigated the significance of benzoic acid as an anchoring group rather than the corresponding carboxylic acid without a phenyl spacer, particularly, when BTD is used as an electron acceptor, for obtaining higher power-conversion efficiencies in the dye-sensitized solar cells.

In this study, BTD was employed as the π-conjugated linker between the porphyrin core and the anchoring group. The anchoring group was chosen to be a simple carboxylic acid group or benzoic acid, and the two new dyes **GY21** and **GY50** (Scheme 1) were synthesized (see the Supporting Information for details). The absorption spectra of these two porphyrin dyes were measured in tetrahydrofuran (THF) solvent (see Figure S1 and Table S1 in the Supporting Information). Both porphyrins exhibited absorption maxima in the 400–500 and 600–750 nm range, which correspond to the Soret and Q band, respectively, whereby **GY50** showed a slightly higher molar absorption coefficient than that of **GY21**. The Soret band of **GY50** is slightly red-shifted with

[*] A. Yella,[+] S. M. Zakeeruddin, M. Grätzel
Laboratory for Photonics and Interfaces
Institute of Chemical Sciences and Engineering
École Polytechnique Fédérale de Lausanne
1015 Lausanne (Switzerland)
E-mail: michael.graetzel@epfl.ch
C.-L. Mai,[+] S.-N. Chang, C.-H. Hsieh, C.-Y. Yeh
Department of Chemistry and Center of Nanoscience and Nanotechnology, National Chung Hsing University
Taichung 402 (Taiwan)
E-mail: cyyeh@dragon.nchu.edu.tw
[+] These authors contributed equally.

[**] M.G. thanks the European Research Council for an Advanced Research Grant (ARG 247404) funded under the "MESOLIGHT" project and the European Community's Seventh Framework Programme for funding under the "GLOBASOL" project. C.-Y.Y. is grateful for the financial support of the National Science Council of Taiwan and the Ministry of Education of Taiwan.
Supporting information for this article is available on the WWW under http://dx.doi.org/10.1002/anie.201309343.

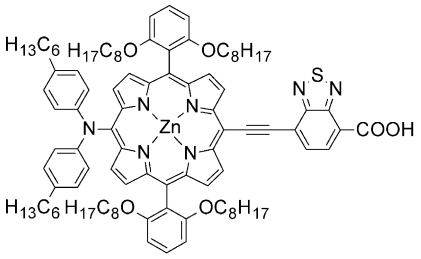

GY21

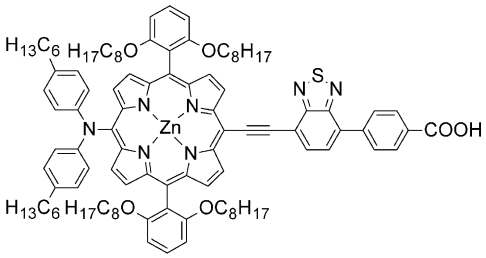

GY50

Scheme 1. Structure of the two dyes used in this study.

respect to that of **GY21**, and its Q-band is narrower than that of **GY21**. This difference is ascribed to the effect of the electron-withdrawing BTD moiety as a π-conjugated linker between the porphyrin and the anchoring group. When the BTD moiety is directly attached to the carboxylic acid (as in the case of **GY21**), the electron-withdrawing effect is higher, thus resulting in a red shift in the Q-band as compared to that of **GY50**, which has a benzoic acid anchoring group. In the latter case, the electronic coupling is attenuated owing to the lack of planarity between the BTD and phenyl rings. The emission behavior for the two sensitizers matches their absorption spectra, with the fluorescence maximum of **GY50** blue-shifted by about 60 nm relative to that of **GY21**. The oxidation potentials of the two dyes were determined by means of cyclic voltammetry (CV). **GY50** showed two oxidation waves at half-wave potential $E_{1/2} = +0.79$ and $+1.22$ V versus the normal hydrogen electrode (NHE; see Figure S2). These values are lower than the corresponding potentials of **GY21** (see Table S1) because of the presence of the phenyl ring between the BTD moiety and the carboxylic acid. The 50 mV negative shift of the reduction potential of **GY50** corresponds to a lifting of the level of the lowest unoccupied molecular orbital (LUMO) and is a result of the same effect.

The photovoltaic performance of the two dyes **GY50** and **GY21** was evaluated by using them in DSCs with a redox mediator based on cobalt tris(bipyridine) in acetonitrile. The current–voltage (J–V) characteristics of these devices under simulated one-sun illumination (AM 1.5 G, 100 mW cm^{-2}) are presented in Figure 1 a, and the corresponding photovoltaic data are summarized in Table 1. The short-circuit current density (J_{SC}) obtained in the case of **GY21** is dramatically lower than that of **GY50**, despite the fact that **GY21** possesses a 10 nm red-shift in the absorption spectrum as compared to **GY50**. Even though a blue shift in the Q-band maximum was observed with the **GY50** sensitizer, the best dye solar cell made with this dye resulted in a J_{SC} value as high as

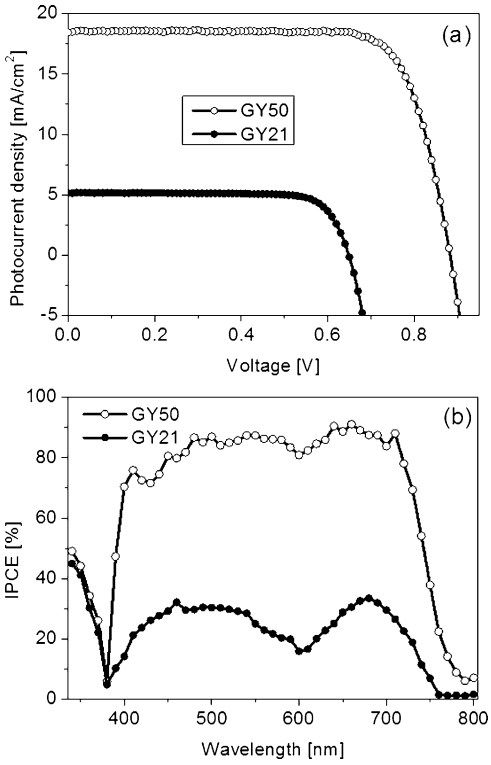

Figure 1. a) J–V characteristics of the devices made with the **GY50** and **GY21** dyes by using a cobalt tris(bipyridine) redox electrolyte. b) Photocurrent action spectrum (IPCE) of the same devices made with **GY50** and **GY21**.

Table 1: Detailed photovoltaic parameters obtained with the **GY50** and **GY21** dyes by using a cobalt tris(bipyridine) redox electrolyte.

Dye	Redox couple	Power [mW cm^{-2}]	V_{OC} [mV]	J_{SC} [mA cm^{-2}]	FF	PCE [%]
		97.8	615	5.03	0.798	2.52
GY21	Co^{2+}/Co^{3+}	50.8	597	2.62	0.80	2.48
		9.5	549	0.47	0.797	2.17
		99.5	885	18.53	0.773	12.75
GY50	Co^{2+}/Co^{3+}	51.0	865	9.78	0.795	13.15
		9.6	809	1.84	0.80	12.5

18.3 mA cm^{-2}, as opposed to a value of approximately 5.5 mA cm^{-2} observed in the case of **GY21**. The open-circuit potential (V_{OC}) of the devices made with **GY21** was only about 615 mV. The introduction of the phenyl spacer in between the anchoring group and the BTD moiety produced a striking enhancement of V_{OC} to around 885 mV. Both devices have similar fill-factor (FF) values. Overall, **GY21** gave a solar-to-electric power-conversion efficiency (PCE) of 2.5%, as compared to 12.75% for **GY50**. The 5.1-fold increase resulted from the cumulative augmentation of V_{OC} and J_{SC}. This PCE achieved with a single dye exceeds our previous record efficiency of 12.3%, which was reached with a push–pull porphyrin dye coded YD2-o-C8 when cosensitized with an organic D–π-A sensitizer. The high efficiency was maintained also at lower 0.5 and 0.1 sun intensities. The

complete *J–V* details at different solar-light intensities for the two dyes are given in Table 1. A histogram of the PCE of approximately 100 devices at full sun intensity and at 64% sun intensity is shown in Figure S5 of the Supporting Information. Higher average PCEs were obtained at 64% sun intensity than at full sun intensity. Since the current densities obtained in the case of the **GY50** dye were more than 18 mA cm^{-2}, some mass-transport limitations of the cobalt redox mediators were encountered at full sun intensity. One of the **GY50** dye devices was sent to an accredited photovoltaic calibration laboratory for certification and reached a PCE of 11.74%, as measured under standard AM 1.5 G reporting conditions (see Figure S6 for the *J–V* characteristics and IPCE spectral response).

Figure 1b shows the incident-photon-to-current conversion efficiency (IPCE) as a function of excitation wavelength for the sensitizers **GY21** and **GY50.** The IPCE spectra of the devices made with these two dyes closely follow the absorption spectrum of the sensitized TiO_2 layer. Both dyes exhibited an IPCE onset at around 790 nm (Figure 1b). The IPCE spectrum of **GY21** showed two maxima at approximately 480 and 700 nm attributed to the Soret band and Q-band absorption, respectively, which attained around 35%. By contrast, **GY50** maintained a much higher IPCE value of 85% across the whole visible wavelength range from 450 to 760 nm, even though both dyes exhibited similar molar absorptivity. The J_{SC} values derived from the overlap integral of the photocurrent action spectra agree within 2% with the measured J_{SC} values, thus showing that the spectral mismatch between the simulator and the true AM 1.5 emission is small.

Cosensitization with the organic dyes, which has complementary absorption, was employed previously[26] to enhance the J_{sc} value by filling the absorption gap between the Soret and Q-bands. In the case of **GY50**, it is evident from the IPCE that the broadening of the Soret band had the same effect, thus rendering the use of a cosensitizer superfluous. This characteristic is advantageous, as the use of cosensitizers often reduces the V_{oc} value.

To confirm the importance of combining cobalt-based redox couples with the porphyrin dyes, an iodine electrolyte consisting of 1-methyl-3-propylimidazolium iodide (PMII; 1M), iodine (60 mM), 4-*tert*-butylpyridine (0.5M), and lithium bis(trifluoromethanesulfonyl)imide (0.1M) in acetonitrile was used to fabricate iodide/triiodide redox-electrolyte-based cells. The photocurrent action spectra of the iodine cells exhibited a similar pattern to that observed for the cobalt counterparts (Figure 2b). The *J–V* characteristics of these iodine cells under full sunlight are also included in Figure 2 for comparison, and the detailed photovoltaic parameters are listed in Table 2. Regardless of the electrolyte, the **GY50** dye displayed a better cell efficiency and better IPCE, thus substantiating the superiority of the use of the phenyl spacer (in between BTD and the carboxylic acid group) in the dyes containing the BTD acceptor group.

The IPCE value is determined on the basis of four factors: light-harvesting efficiency (LHE), the injection efficiency of the dye into the conduction band, regeneration efficiency, and charge-collection efficiency. These four factors were examined separately to find out the reasons for the much higher

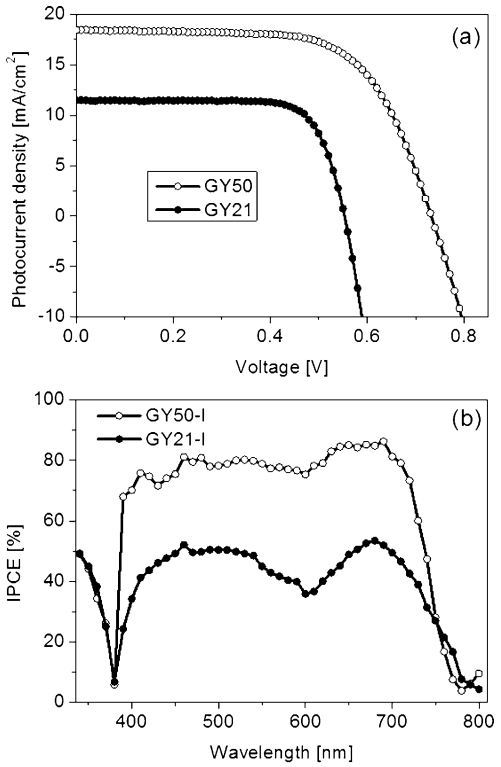

Figure 2. a) *J–V* characteristics of the devices made with the **GY50** and **GY21** dyes by using a iodide/triiodide redox electrolyte. b) Photocurrent action spectrum (IPCE) of the same devices made with **GY50** and **GY21**.

Table 2: Detailed photovoltaic parameters obtained with the **GY50** and **GY21** dyes by using an iodide/triiodide redox electrolyte.

Dye	Redox couple	Power [mW cm^{-2}]	V_{OC} [mV]	J_{SC} [mA cm^{-2}]	FF	PCE [%]
		9.7	486	1.14	0.765	4.35
GY21	I^-/I_3^-	51.6	536	5.99	0.764	4.75
		98.8	552	11.50	0.751	4.84
		9.5	688	1.83	0.715	9.54
GY50	I^-/I_3^-	51.2	721	9.70	0.684	9.35
		99.7	732	18.45	0.657	8.90

IPCE values obtained with **GY50** as compared to those obtained with **GY21**. The LHE of a 3 μm transparent TiO_2 film sensitized with the two dyes is shown in Figure 3. The LHE of the two dyes **GY50** and **GY21** was very similar and exhibited maxima that correlated with the Soret and Q bands of the porphyrins. The LHE reached near-unity in both cases, from which we can rule out the possibility that the change in the LHE causes any difference in the IPCE of the **GY50** and **GY21** porphyrins.

We carried out time-resolved fluorescence measurements on the **GY50** and **GY21** dyes to see if the difference in the injection efficiency of these two dyes could account for the difference in the IPCE. Figure S7 in the Supporting Information shows the time-resolved luminescence of the two dyes **GY50** and **GY21** in ethanolic solution and adsorbed on 3 μm

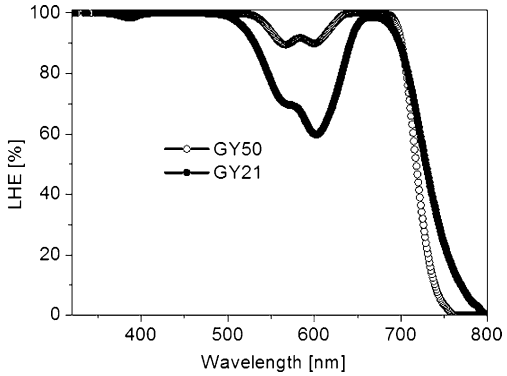

Figure 3. Light-harvesting efficiency (LHE) of the two dyes **GY50** and **GY21** on a 3 μm transparent TiO_2 film.

transparent TiO_2 and Al_2O_3 films. In solution, the fluorescence lifetime was 1.3 ns in both cases. When the two dyes were grafted on the aluminum oxide, the fluorescence decayed more rapidly (ca. 750 ps) than in solution. However, when adsorbed on a TiO_2 film, the emission decay of the two dyes was further enhanced. This result is indicative of efficient photoinduced electron injection from the dye into the mesoporous TiO_2 film.

To determine if there was any difference in the regeneration of the two dyes, we carried out photoinduced-absorption measurements in the presence and in the absence of the redox electrolyte (see Figure S8). In the absence of the redox electrolyte, the absorption peaks at 800 and 1300 nm confirmed the presence of the porphyrin radical cation formed by the injection of an electron into the conduction band of titania. In the presence of the redox electrolyte (either the iodide- or the cobalt-based redox electrolyte), the two features completely disappeared, thus indicating the regeneration of the dye cation by the redox mediator. Since the differences in the LHE, electron injection, and dye regeneration are negligible between the two dyes **GY50** and **GY21**, the difference in the IPCE is likely to be the result of the difference in collection efficiency in these two cases.

To clarify this assumption, we measured transient photocurrent and photovoltage decay to determine the lifetime of the injected electrons from TiO_2 to the electrolyte. Figure 4 shows the lifetime of the electrons in the TiO_2 film within the device as a function of the charge density for the two dyes with a cobalt redox mediator. The electron lifetime in the case of **GY50** was 100 times longer than that for **GY21**. At each particular charge density, the electrons in the conduction band for devices made with **GY21** recombined 100 times faster with the cobalt electrolyte than in devices sensitized with **GY50**. The recombination rate in the case of **GY21** was also higher when the cobalt redox electrolyte was replaced with the iodide-based redox electrolyte. Figure 4b shows the lifetime of the electrons for the two dyes with the iodide/triiodide redox couple.

The lower V_{OC} value in the case of the devices sensitized with **GY21** can be attributed to the downward shift of the conduction band of the titania. Since the chemical capacitance (C_μ) is directly proportional to the density of states in the TiO_2 film, lower C_μ values indicate an upward shift in the

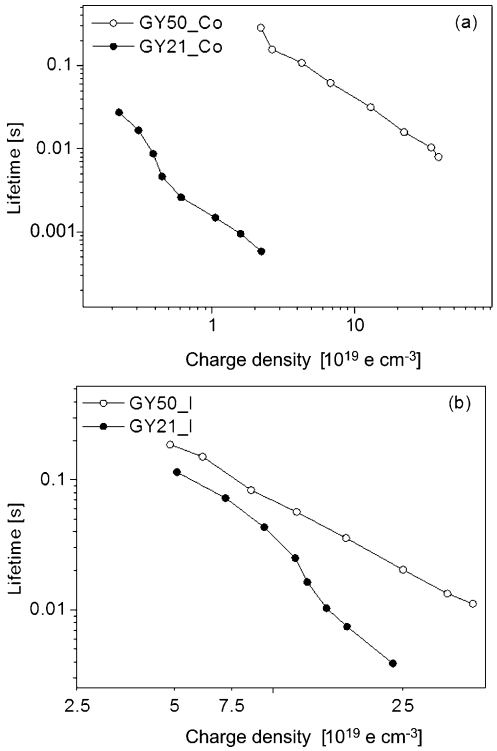

Figure 4. Electron lifetime as a function of charge density for the **GY50** and **GY21** dyes with a) a cobalt tris(bipyridine) redox electrolyte and b) an iodide/triiodide redox electrolyte.

density of states as compared to the other dye. Figure S9 in the Supporting Information shows the density of states (DOS) versus charge density for devices sensitized with **GY21** and **GY50**. In the case of films sensitized with **GY21**, the trap states were much deeper than those of devices sensitized with **GY50**. Therefore, it can be concluded that the dramatic increase of 270 mV in the V_{OC} value is a cumulative effect caused by the increase in the electron lifetime as well as the upward shift in the trap-state distribution upon the adsorption of **GY50**.

We also measured the photocurrent decay under short-circuit conditions to analyze the dynamics of the electron-transport process. The collection efficiency is the ratio between the transport rate and the sum of recombination and transport rates. In the case of the **GY50** dye, the collection efficiency was more than 90% at all charge densities, whereas in the case of **GY21**, the collection efficiency dropped to 50% as the charge density increased (see Figure S9). The same relationships were observed for both the iodide and the cobalt electrolyte system. Hence, the lower power-conversion efficiency and the lower IPCE in the case of **GY21** can be attributed to its poor charge-collection efficiency.

In conclusion, we have shown the importance of introducing a phenyl group between the BTD and carboxylic acid groups of a zinc porphyrin dye for high power-conversion efficiency. The addition of the BTD moiety resulted in the filling of the gap between the Soret band and the Q band in the IPCE, which eliminated the need to use a complementary

dye for cosensitization; the observed efficiency is the highest found for a single zinc porphyrin dye. Besides the filling of this gap, a red shift was observed as compared to previously reported dyes owing to the strong withdrawing nature of the BTD group. Although the presence of the phenyl group resulted in a slight blue shift in the absorption spectrum, it reduced recombination by a factor of 100 in the case of a cobalt-based redox electrolyte and by a factor of 10 in the case of an iodide-based redox electrolyte. Not only was recombination higher in the absence of the phenyl group, but the chemical capacitance was also higher, thus resulting in deeper trap states and in turn a lower V_{oc} value. By careful engineering of the dye structure, a fivefold increase in efficiency was observed.

Received: October 26, 2013
Revised: January 6, 2014
Published online: February 5, 2014

Keywords: dyes · energy conversion · porphyrinoids · sensitizers · solar cells

[1] M. Grätzel, *Nature* **2001**, *414*, 338 – 344.
[2] F. Gao, Y. Wang, D. Shi, J. Zhang, M. Wang, X. Jing, R. Humphry-Baker, P. Wang, S. M. Zakeeruddin, M. Grätzel, *J. Am. Chem. Soc.* **2008**, *130*, 10720 – 10728.
[3] C. Chen, M. Wang, J. Li, N. Pootrakulchote, L. Alibabaei, C. Ngoc-le, J. Decoppet, J. Tsai, C. Grätzel, C. Wu, S. M. Zakeeruddin, M. Grätzel, *ACS Nano* **2009**, *3*, 3103.
[4] Q. Yu, Y. Wang, Z. Yi, N. Zu, J. Zhang, M. Zhang, P. Wang, *ACS Nano* **2010**, *4*, 6032.
[5] Y. Chiba, A. Islam, Y. Watanabe, R. Komiya, N. Koide, L. Y. Han, *Jpn. J. Appl. Phys. Part 2* **2006**, *45*, L638 – L640.
[6] R. Komiya, A. Fukui, N. Murofushi, N. Koide, R. Yamanaka, H. Katayama, Improvement of the Conversion Efficiency of a Monolithic Type Dye-Sensitized Solar Cell Module, Technical Digest, 21st International Photovoltaic Science and Engineering Conference, Fukuoka, November **2011**, 2 C-50-08.
[7] G. Zhang, H. Bala, Y. Cheng, D. Shi, X. Lv, Q. Yu, P. Wang, *Chem. Commun.* **2009**, 2198 – 2200.
[8] W. Zeng, Y. Cao, Y. Bai, Y. Wang, Y. Shi, M. Zhang, F. Wang, C. Pan, P. Wang, *Chem. Mater.* **2010**, *22*, 1915 – 1925.
[9] S. Ito, H. Miura, S. Uchida, M. Takata, K. Sumioka, P. Liska, P. Comte, P. Pechy, M. Grätzel, *Chem. Commun.* **2008**, 5194.
[10] R. Li, J. Liu, N. Cai, M. Zhang, P. Wang, *J. Phys. Chem. B* **2010**, *114*, 4461.
[11] W. Zhu, Y. Wu, S. Wang, W. Li, X. Li, J. Chen, Z.-S. Wang, H. Tian, *Adv. Funct. Mater.* **2011**, *21*, 756.
[12] M. M.-D. Victoria, G. D. L. Torre, T. Torres, *Chem. Commun.* **2010**, *46*, 7090.
[13] H. Imahori, T. Umeyama, S. ITO, *Acc. Chem. Res.* **2009**, *42*, 1809.
[14] M. G. Walter, A. B. Rudine, C. C. Wamser, *J. Porphyrins Phthalocyanines* **2010**, *14*, 759.
[15] Y. Liu, H. Lin, J. T. Dy, K. Tamaki, J. Nakazaki, D. Nakayama, S. Uchida, T. Kubo, H. Segawa, *Chem. Commun.* **2011**, *47*, 4010.
[16] H. Imahori, Y. Matsubara, H. Iijima, T. H. Umeyama, Y. Matano, S. Ito, M. Niemi, N. V. Tkachenko, H. Lemmetyinen, *J. Phys. Chem. C* **2010**, *114*, 10656.
[17] Y. Wang, X. Li, B. Liu, W. Wu, W. Zhua, Y. Xie, *RSC Adv.* **2013**, *3*, 14780 – 14790.
[18] T. Ripolles-Sanchis, B.-C. Guo, H.-P. Wu, T.-Y. Pan, H.-W. Lee, S. R. Raga, F. Fabregat-Santiago, J. Bisquert, C.-Y. Yeh, E. W.-G. Diau, *Chem. Commun.* **2012**, *48*, 4368 – 4370.
[19] D. Kiessling, R. D. Costa, G. Katsukis, J. Malig, F. Lodermeyer, S. Feihl, A. Roth, L. Wibmer, M. Kehrer, M. Volland, P. Wagner, G. G. Wallace, D. L. Officer, D. M. Guldi, *Chem. Sci.* **2013**, *4*, 3085.
[20] T. Bessho, S. M. Zakeeruddin, C.-Y. Yeh, E. W.-G. Diau, M. Grätzel, *Angew. Chem.* **2010**, *122*, 6796 – 6799; *Angew. Chem. Int. Ed.* **2010**, *49*, 6646 – 6649.
[21] C.-P. Hsieh, H.-P. Lu, C.-L. Chiu, C.-W. Lee, S.-H. Chuang, C.-L. Mai, W.-N. Yen, S.-J. Hsu, E. W.-G. Diau, C.-Y. Yeh, *J. Mater. Chem.* **2010**, *20*, 1127 – 1134.
[22] Y.-C. Chang, C.-L. Wang, T.-Y. Pan, S.-H. Hong, C.-M. Lan, H.-H. Kuo, C.-F. Lo, H.-Y. Hsu, C.-Y. Lin, E. W.-G. Diau, *Chem. Commun.* **2011**, *47*, 8910 – 8912.
[23] M. Ishida, D. Hwang, Y. B. Koo, J. Sung, D. Y. Kim, J. L. Sessler, D. Kim, *Chem. Commun.* **2013**, *49*, 9164 – 9166.
[24] M. S. Kang, I. T. Choi, Y. W. Kim, B. S. You, S. H. Kang, J. Y. Hong, M. J. Ju, H. K. Kim, *J. Mater. Chem. A* **2013**, *1*, 9848 – 9852.
[25] P. K. B. Palomaki, M. R. Civic, P. H. Dinolfo, *ACS Appl. Mater. Interfaces* **2013**, *5*, 7604 – 7612.
[26] A. Yella, H.-W. Lee, H. N. Tsao, C. Yi, A. K. Chandiran, M. K. Nazeeruddin, E. W.-G. Diau, C.-Y. Yeh, S. M. Zakeeruddin, M. Grätzel, *Science* **2011**, *334*, 629 – 634.
[27] S. Haid, M. Marszalek, A. Mishra, M. Wielopolski, J. Teuscher, J. E. Moser, R. Humphry-Baker, S. M. Zakeeruddin, M. Grätzel, P. Bäuerle, *Adv. Funct. Mater.* **2012**, *22*, 1291.

